AD-A140 549 FUNDAMENTAL PROCESSES IN PARTIALLY IONIZED PLASMAS(U) 1/1
STANFORD UNIV CA HIGH TEMPERATURE GASDYNAMICS LAB
C H KRUGER ET AL. FEB 84 AFOSR-TR-84-0257 AFOSR-83-0108
UNCLASSIFIED F/G 20/9 NL

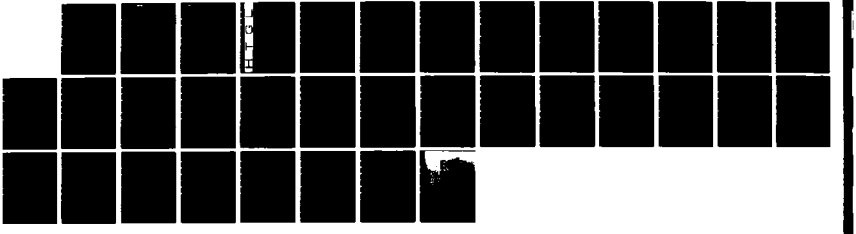

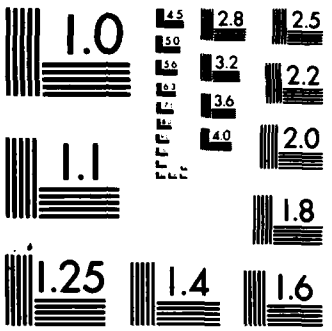

SECURITY CLASSIFICATION OF THIS PAGE (When Data Entered)

UNCLASSIFIED

REPORT DOCUMENTATION PAGE

READ INSTRUCTIONS BEFORE COMPLETING FORM

1. REPORT NUMBER: AFOSR-TR- 84-0257	2. GOVT ACCESSION NO.
3. RECIPIENT'S CATALOG NUMBER	4
4. TITLE (and Subtitle): Fundamental Processes in Partially Ionized Plasmas	5. TYPE OF REPORT & PERIOD COVERED: Annual Scientific Report Feb. 1, 1983 to Jan. 31, 1984
	6. PERFORMING ORG. REPORT NUMBER
7. AUTHOR(s): C. H. Kruger, Principal Investigator M. Mitchner, Co-Principal Investigator S. A. Self, Co-Principal Investigator	8. CONTRACT OR GRANT NUMBER(s): Grant AFOSR-83-0108
9. PERFORMING ORGANIZATION NAME AND ADDRESS: Stanford University Mechanical Engineering Department Stanford, CA 94305	10. PROGRAM ELEMENT, PROJECT, TASK AREA & WORK UNIT NUMBERS: 61102F 2301/A8
11. CONTROLLING OFFICE NAME AND ADDRESS: Dr. Henry Radoski, Directorate of Physics AFOSR/NP, Bolling AFB, Building 410 Washington, DC 20332	12. REPORT DATE: February 1984 13. NUMBER OF PAGES: 31
14. MONITORING AGENCY NAME & ADDRESS (if different from Controlling Office)	15. SECURITY CLASS. (of this report): unclassified 15a. DECLASSIFICATION/DOWNGRADING SCHEDULE: N/A

16. DISTRIBUTION STATEMENT (of this Report)

Approved for public release; distribution unlimited.

17. DISTRIBUTION STATEMENT (of the abstract entered in Block 20, if different from Report)

18. SUPPLEMENTARY NOTES

APR 26 1984

19. KEY WORDS (Continue on reverse side if necessary and identify by block number)

Plasma	Sheath	Secondary flow	Turbulence-dampening
Ionized	Weakly-ionized	Power	Anode
Recombination	Boundary layer	Hartmann	Cathode
Three-body	Magnetohydrodynamic	Diagnostics	Electrothermal
Discharge	MHD	Propulsion	Breakdown

20. ABSTRACT (Continue on reverse side if necessary and identify by block number)

This report describes progress during the first year of a research program on the Fundamental Processes in Partially Ionized Plasmas conducted in the High Temperature Gasdynamics Laboratory at Stanford University. This research is directed to three major areas: recombination in molecular plasmas, discharge effects (plasma electrode interaction) and interaction of discharges and fluid dynamics. Recombination and ionization are fundamental processes that play a role in nearly all applications and natural phenomena that involve partially

(continued on reverse side)

DD FORM 1 JAN 73 1473 EDITION OF 1 NOV 65 IS OBSOLETE

UNCLASSIFIED

SECURITY CLASSIFICATION OF THIS PAGE (When Data Entered)

84 04 24

BLOCK 20 (Abstract) continued

ionized plasmas. Under the present program, experiments have been designed and theoretical analyses conducted to obtain a better knowledge of the rates of electron recombination in the presence of molecular species. Studies have been initiated of the near-electrode region and the processes by which current is transferred between the plasmas and the electrodes. The first stage of theretical modeling of these processes has now been completed and published. A study of the interaction of discharges and fluid dynamics has measured the significant secondary flows caused by the interaction of a magnetic field with a current-carrying plasma. Experimental and theoretical research in each of these areas is continuing.

HTGL

Annual Scientific Report

on

FUNDAMENTAL PROCESSES IN PARTIALLY IONIZED PLASMAS

Grant AFOSR-83-0108

Prepared for

AIR FORCE OFFICE OF SCIENTIFIC RESEARCH

For the Period

February 1, 1983 to January 31, 1984

Submitted by

C. H. Kruger, Principal Investigator
M. Mitchner, Co-Principal Investigator
S. A. Self, Co-Principal Investigator

HIGH TEMPERATURE GASDYNAMICS LABORATORY
Mechanical Engineering Department
Stanford University

Annual Scientific Report

on

FUNDAMENTAL PROCESSES IN PARTIALLY IONIZED PLASMAS

Grant AFOSR-83-0108

Prepared for

AIR FORCE OFFICE OF SCIENTIFIC RESEARCH

For the Period

February 1, 1983 to January 31, 1984

Submitted by

C. H. Kruger, Principal Investigator
M. Mitchner, Co-Principal Investigator
S. A. Self, Co-Principal Investigator

Table of Contents

1.0 INTRODUCTION

This report describes progress during the first year of a research program on the Fundamental Processes in Partially Ionized Plasmas conducted in the High Temperature Gasdynamics Laboratory at Stanford University. This research is supported by a grant from the Air Force Office of Scientific Research (AFOSR-83-0108) and is conducted under the direction of Professors Charles H. Kruger, Morton Mitchner, and Sidney Self. Three Ph.D. candidates are currently conducting their doctoral research under this program.

Several space power and propulsion systems of potential long-range interest to the Air Force involve partially ionized plasmas. Such systems include MPD thrusters, both open and closed cycle MHD power, and thermionic energy conversion. Although the specific configurations, the exact operating conditions, and which of the competing systems will prove to be most useful in the long term remain to be established, it is important at this time to provide a broad fundamental research base in support of development activity. In particular, there are a number of key issues regarding the properties and discharge behavior of partially ionized plasmas and the interaction of discharges with fluid dynamics that need to be understood before the potential and limitations of competing systems can be fully evaluated. In addition, it is important that outstanding young applied scientists be educated in these areas.

The present research on partially ionized plasmas is discipline rather than device oriented and is currently focused on three major areas:

1. Recombination in molecular plasmas
2. Discharge effects: plasma electrode interaction
3. Interaction of discharges and fluid dynamics

In addition, each of these areas involves the development and application of modern plasma diagnostic techniques.

These areas are overlapping and mutually supportive. Thus, understanding of plasma properties is important to the study of discharges and their interaction with fluid dynamics. In the same spirit, we are interested in the development of plasma diagnostics so that they can be applied in our research objectives. In each area, the research is primarily experimental in nature, with supporting theoretical studies for the planning of the research and interpretation of the data.

Progress during the first year in each of the three research areas is described by means of Project Summaries in Section 2.0.

Publications and Presentations resulting from this work are cited in Section 4.0, and Section 5.0 lists the personnel who have contributed to this report.

2.0 PROJECT SUMMARIES

Included in this section are summaries of progress in each of three project areas. Each project summary contains the following subsections: (a) Introduction; (b) Scientific Merit; and (c) Status Report. Additional descriptions may be found in the publications listed in Section 4.0.

2.1 Recombination in Molecular Plasmas

Introduction

The equilibrium thermodynamic properties and the quasi-equilibrium transport properties of partially ionized plasmas have been fairly well worked out, at least with regard to the theoretical aspects, and many important results are given in the book Partially Ionized Gases [1.1]. There remain, however, a number of areas where plasma properties are not now adequately understood, particularly with regard to nonequilibrium plasmas. Since a knowledge of plasma properties is fundamental to any system description, it is important that this area receive appropriate attention.

The electron density is often the single most important thermodynamic property; in many nonequilibrium situations it is determined by finite ionization and recombination rates. These rates in turn depend on the constituents of the gas and the form of nonequilibrium. For example, in our experiments with plasma boundary layers, significant electron-density nonequilibrium can not be adequately explained by use of recombination coefficients α_e that assume only electrons as the third body for recombination (i.e., $e + M^+ + e \rightarrow M + e$, where M^+ and M denote an alkali metal ion and atom, resp.). Existing values of heavy-body recombination coefficient α_j (for $e + M^+ + X_j \rightarrow M + X_j$, where X_j is an atom or molecule) improve the agreement but remain unsatisfactory.

Experimental studies of the recombination process in which the third body is an atom or molecule have been carried out using (hydrocarbon) flames [1.2], where the products of combustion contained several molecular species. To extract information about the individual molecules

X_j, the assumption was made that the contributions from the different molecules in the mixture were additive. Expressed equivalently, in terms of recombination coefficients, it was assumed that the overall rate α (which was measured, in effect) could be written in terms of the individual rates α_j by the formula

$$\alpha = \sum_j x_j \alpha_j \quad ,$$

where $x_j = n_j/n$ denotes the mole fraction of species X_j. Here n_j is the number density of species X_j and n is the total number density.

The results obtained in this fashion have been strongly criticized by Bates [1.3], who claimed that the recombination coefficient for a molecular mixture is <u>not additive</u>, but that it is given by the formula

$$\alpha = \frac{n}{\eta} \left\{ \sum_p \frac{1}{\sum_j x_j B_j(p)} \right\}^{-1} .$$

The quantities $B_j(p)$ are related to the rates of de-excitation of M by X_j from all energy levels above and including p, to all levels below p. The factor η is given in terms of atomic constants and the temperature T as $(2\pi m_e kT/h^2)^{3/2} = KT^{3/2}$.

For a single species, one obtains from this expresison for α the result

$$\alpha_j = \frac{n_j}{\eta} \left\{ \sum_p \frac{1}{B_j(p)} \right\}^{-1} .$$

It is therefore apparent that the value of α for a mixture of molecules cannot be written, in general, in terms of the individual α_j. To be able to calculate α for a mixture, the factors $B_j(p)$ must be used. However before being able to rely on the calculated factors $B_j(p)$, it is necessary to test the theory by obtaining data in which only a single molecular species X_j is present in the recombining gas together with the alkali metal M. It is clear that flame experiments are unable to yield such data.

Scientific Merit

Recombination and ionization are fundamental processes that play a role in nearly all applications and natural phenomena that involve partially ionized plasmas. For nonequilibrium situations, knowledge of the rates for these processes are needed for estimating electron density, and thereby, electrical conductivity. This information is necessary in designing and understanding the performance of new devices, as well as in understanding the nature of many terrestrial and solar phenomena.

Status Report

To achieve conditions necessary for acquiring basic data and for testing Bate's theory, experiments are planned where the basic approach will be to employ a supersonic expansion of a high temperature gas. The experimental apparatus for this work is indicated schematically in Figure 1.1. An arc heater will be used to produce a flow of high

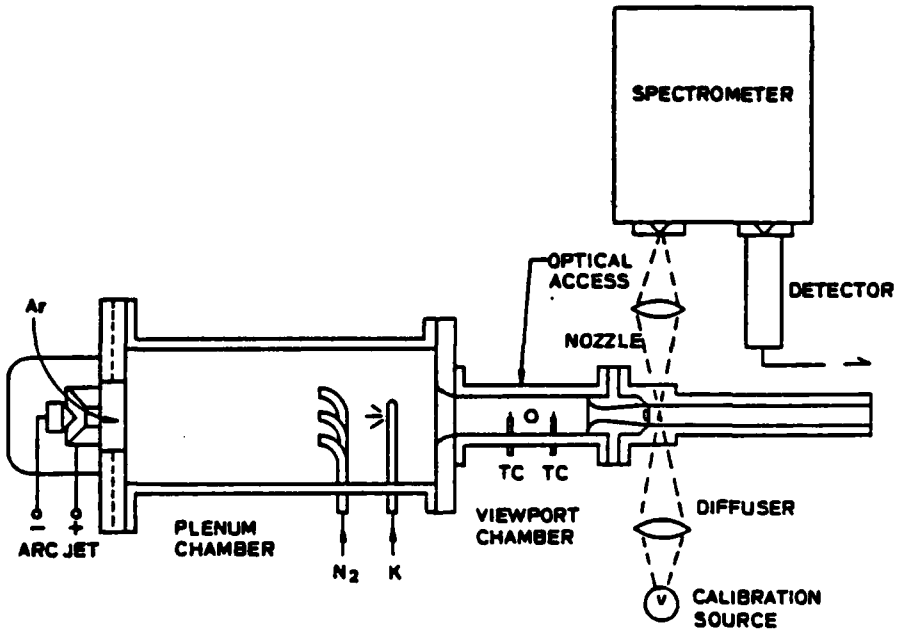

Figure 1.1. Proposed experimental aparatus for measurement of the molecular 3-body recombination coefficient.

temperature Ar into a large plenum chamber. Potassium vapor will be added to the gas, together with various molecular species introduced either singly, or in controlled combinations. The purpose of the plenum is to permit a thorough mixing of the gases and to enable the mixture to come to thermodynamic equilibrium.

The gas mixture then flows through a chamber viewport where the stagnation temperature of the gas can be measured with thermocouples and by spectroscopic methods. A convergent-divergent supersonic nozzle follows, in which the gas will be rapidly cooled, so that electron recombination is induced. The electron number density will be measured spectroscopically at the exit of the nozzle, thereby providing data from which the recombination coefficient can be calculated. The gas will then pass through a supersonic diffuser and be exhausted to the atmosphere.

To design the apparatus, it is necessary to determine approximately the optimal experimental conditions, within the constraints imposed by the operating limits of the arc jet. These conditions include the plenum pressure and temperature, the number densities of the potassium and the molecular gas additives, and the geometry of the converging-diverging nozzle. Since 3-body recombination will occur in which both the electrons and the molecules serve as third bodies, it is desirable that experiments be conducted for conditions such that the latter process is dominant.

At higher pressures, collisional atomic processes dominate radiative processes, so that one may write $\alpha_e = n_e \alpha_e'(T)$ and $\alpha_j = n_j \alpha_j'(T)$, where $\alpha_e'(T)$ and $\alpha_j'(T)$ are functions of temperature. (Here n_e and n_j denote the electron and molecular number densities.) Shown in Figure 1.2, are the values of α_{N_2}' for N_2, as calculated by Bates, Malaviya, and Young [1.4], and the values of α_e' as given by Hinnov and Hirschberg [1.5]. We shall take N_2 as the molecular third body in the discussion that follows.

The quasi one-dimensional steady state electron continuity equation that governs the behavior of n_e, is

$$u \frac{dn_e}{dx} + n_e \frac{du}{dx} + u n_e \frac{d}{dx} \ell n\, A = \dot{n}_e \ ,$$

where $\dot{n}_e$ denotes the net electron production rate, and is given by the expression

$$\dot{n}_e = (n_K s - n_e^2)\ (n_e \alpha_e' + n_{N_2} \alpha_{N_2}')\ .$$

Here $s=s(T) = KT^{3/2} \exp(-\varepsilon_i/kT)$, where ε_i is the ionization energy of potassium. In obtaining $\dot{n}_e$, the ionization rates have been expressed as $S_e = s(T)\ \alpha_e'$ and $S_{N_2} = s(T)\ \alpha_{N_2}'$ by use of the method of detailed balancing. The gas flow speed u (as well as all other gas properties) is given in terms of the cross-sectional area of the nozzle $A = A(x)$, by the well-known relations of gas dynamics [1.6].

Before discussing some of the results of integrating the continuity equation for the $n_e(x)$, it is useful to introduce two concepts that serve as a guide in selecting the initial condition at the entrance to the nozzle. We denote the ratio of the recombination rate by N_2 to that by electrons as $r \equiv n_{N_2}\ \alpha_{N_2}'/(n_e \alpha_e')$, and the ratio of the characteristic time for recombination by N_2 to the residence time of a fluid element in the nozzle as $\tau \equiv \tau_{N_2}/\tau_{res}$. Here $\tau_{N_2} \approx (\alpha_{N_2}' n_{N_2} n_e)^{-1}$ and $\tau_{res} \approx L/a$, where L is the nozzle length and $a = (\gamma RT)^{1/2}$ is the speed of sound.

We would anticipate that desirable upstream gas states would satisfy the conditions $r \gtrsim 1$ and $\tau \sim 1$. (For $\tau \ll 1$ the flow would approach the "equilibrium" limit, in which ionization and recombination rates are approximately equal. For $\tau \gg 1$ the flow would be approximately "frozen", where little recombination by N_2 occurs.) The condition on r would ensure that recombination rate by N_2 would exceed that by electrons.

From the equation defining r we may write

$$n_e = \frac{n_{N_2} (\alpha_{N_2}'/\alpha_e')}{r}\ ,$$

and substituting for n_e in the equation defining τ, we obtain

$$n_{N_2} = \left[\left(\frac{r}{\tau}\right) \frac{(\alpha_e'/\alpha_{N_2}')}{\alpha_{N_2}'} 200 \sqrt{T}\ \right]^{1/2}\ .$$

(We have used here the approximate expression $\tau_{res} = 0.005/\sqrt{T}$, corresponding to a nozzle length of 0.1m.) Shown in Figure 1.2 are the values of n_{N_2} plotted as a function of temperature for values of the parameter (r/τ) equal to 1 and 10, and the corresponding values of n_e for r = 1 and 10. Also shown are constant partial pressure lines for N_2 and K with p_{N_2} = 6 atm and p_K = 0.1 atm. These values are estimates of the approximate maximum values of the nitrogen and potassium partial pressures that can be used with the available experimental facilities.

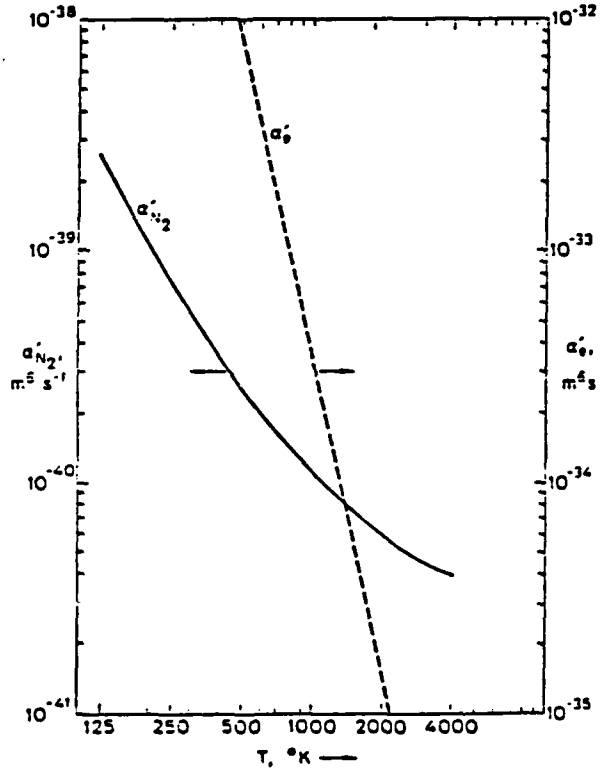

Figure 1.2. Temperature dependence of the 3-body recombination coefficients with either N_2 or electrons serving as the third body

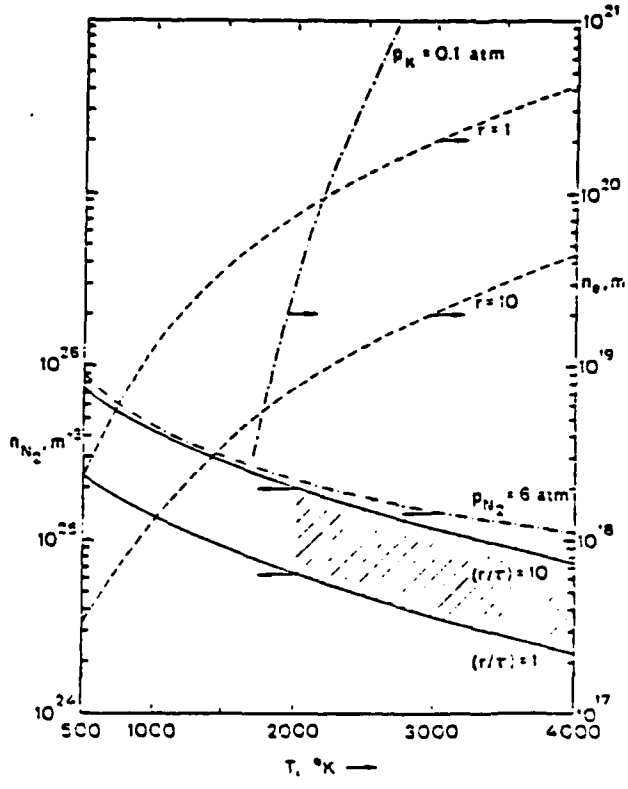

Figure 1.3. Domain of experimental conditions required for determing the 3-body recombination coefficient with N_2.

The estimated range of possible experimental values for n_{N_2} and the temperature fall in the region defined by $T \gtrsim 2000°K$ and by the curves labeled $(r/\tau) = 1$ and $p_{N_2} = 6$ atm. It appears that values of (r/τ) up to about 10 can be achieved, which should be adequate.

To obtain a more accurate picture than is provided by the preceding analysis, a program has been written to integrate the electron continuity equation numerically. It is intended that this program be employed to estimate the optimal experimental conditions that should be used for determining $\alpha'_{N_2}(T)$. The variation of n_e with streamwise location in the nozzle is shown in Figures 1.4 and 1.5 for several gas conditions. The nozzle, in all cases, was assumed to be conical with a half-angle of 3.2° for the converging part, and 1.3° for the diverging part. The four curves in each figure show the "frozen" flow, the "equilibrium" flow, the recombining flow, and the contribution to the recombination by just the electron 3-body process. Figures 1.4 and 1.5 are for stagnation temperatures of 2000°K and 3000°K respectively. With reference to Figure 1.4a, Figure 1.4b shows the effect of increasing n_{N_2}, and Figure 1.4c shows the effect of increasing n_e. With reference to Figure 1.5a, Figure 1.5b shows the effect of increasing n_{N_2}, and Figure 1.5c shows the effect of decreasing n_e.

The term "N_2 effect" for each figure is the fractional decrease in n_e attributable to 3-body recombination with N_2. These results show that increasing the values of n_{N_2} and n_e are generally favorable and increasing T is unfavorable with respect to increasing the fractional effect of N_2. Work is in progress to explore systematically the variation of electron density for various gas conditions and nozzle geometries.

Future work on the mathematical modeling of the recombination process in a rapid expansion will include the following: The model will be used to estimate the accuracy with which the planned experiments can determine the 3-body recombination coefficient, and possible diagnostic methods for measuring n_e will be examined. In addition, the model will be improved to account for skin friction, heat transfer, and the possibility that the electron temperature may differ from the gas temperature. Experimental work will be undertaken to map out the operating

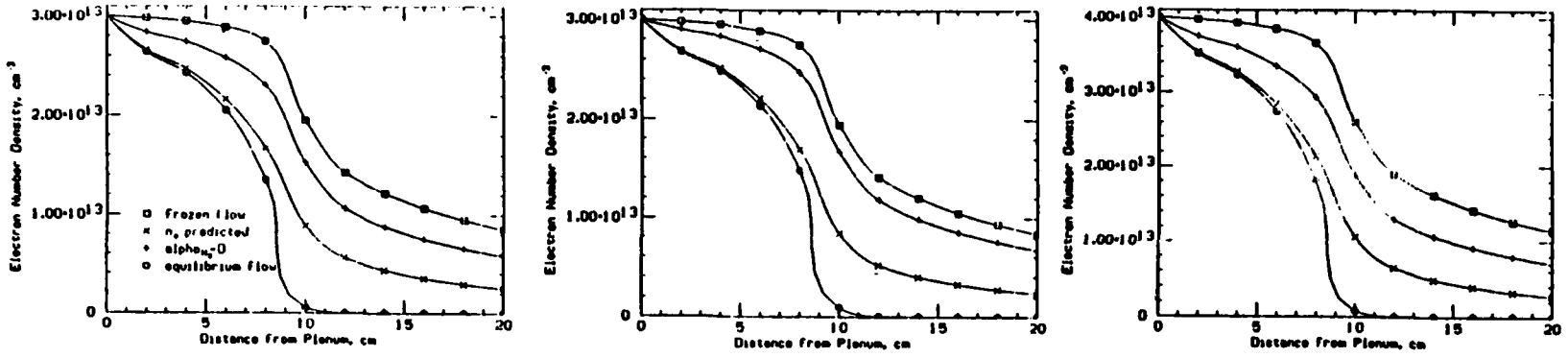

(a) $n_{H_2} = 10^{25} m^{-3}$, $n_e = 3 \times 10^{19} m^{-7}$ (b) $n_{H_2} = 2 \times 10^{25}$, m^{-3}, $n_e = 3 \times 10^{19} m^{-3}$ (c) $n_{H_2} = 10^{25} m^{-3}$, $n_e = 4 \times 10^{19} m^{-3}$

N_2 effect = 1.32 N_2 effect = 1.86 N_2 effect = 1.57

Figure 1.4 Variation of electron density through the nozzle for a stagnation temperature of 2000°K.

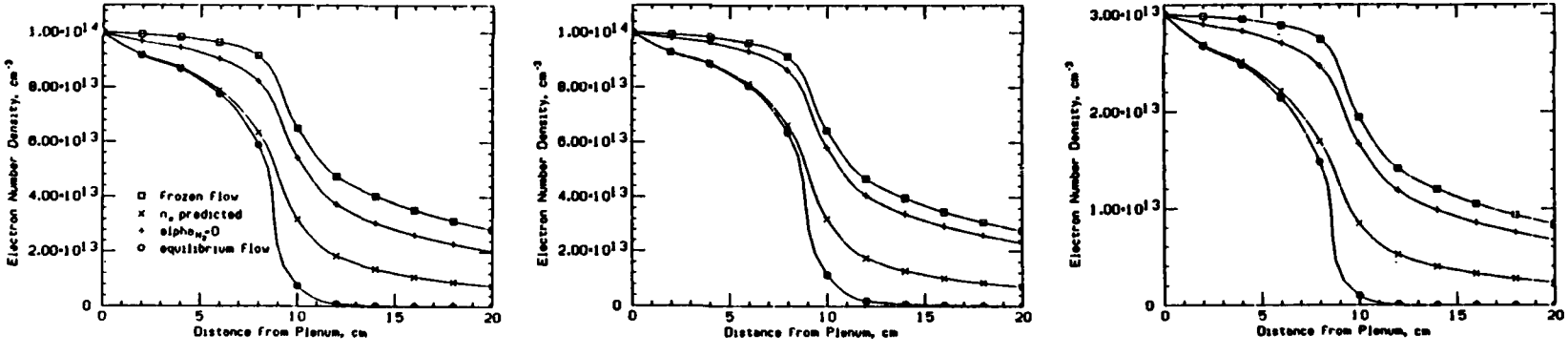

(a) $n_{N_2} = 10^{25} m^{-3}$, $n_e = 10^{20} m^{-3}$ (b) $n_{N_2} = 2 \times 10^{25} m^{-3}$, $n_e = 10^{20} m^{-3}$ (c) $n_{N_2} = 10^{25} m^{-3}$, $n_e = 4 \times 10^{-19} m^{-3}$

N_2 effect = 1.70 N_2 effect = 2.26 N_2 effect = 0.88

Figure 1.5 Variation of electron density through the nozzle for a stagnation temperature of 3000°K.

characteristics of the arc jet for the domain of gas conditions indicated by the theory.

2.2 Discharge Effects: Plasma-Electrode Interaction

Introduction

Insofar as practical applications of plasmas invariably involve the transfer of current between electrodes and the plasma, and since the performance of plasma devices is commonly limited by mechanisms associated with this current transfer, a better understanding of the basic physical processes involved in the plasma-electrode interaction is highly desirable. Among these limiting mechanisms particular reference should be made to the excess voltage drop and power dissipation in the plasma-sheath boundary layer, and the electrode erosion associated with current concentrations at both cathodes and anodes.

The work described under this heading is directed towards providing a more complete understanding of the plasma-electrode interaction for the case of flowing, seeded, thermal plasmas at pressures of the order of one atmosphere, and involves both theoretical and experimental components.

Consider a channel flow of thermal plasma which might be either a noble gas or combustion products gas seeded to a suitable level ($\sim$ 1%) with cesium or potassium. We may define the electric boundary layer as that region near the channel walls, composed of high temperature insulators and electrodes, where charged particle nonequilibrium effects become significant and even dominant. Normally, the walls have to be operated at temperatures less than that of the core flow plasma because of material limitations.

On physical and dimensional grounds the region between the core plasma and the electrode surface can be divided into a number of overlapping layers of decreasing scale. Proceeding from the core plasma to the electrode these layers may be listed as follows (see Figure 2.1).

(1) The gasdynamic boundary layer of scale $\delta \sim 10^{-2}$m

(ii) The ionization nonequilibrium (or ambipolar diffusion) layer of scale ℓ_R, the characteristic recombination length.

(iii) The sheath of scale equal to the Debye length λ_D, typically 10^{-6}m.

(iv) The Knudsen layer where free molecule flow takes over from a continuum (fluid) description and the appropriate scale is the mean free path $\ell_e \sim \ell_i \sim 10^{-6}$m.

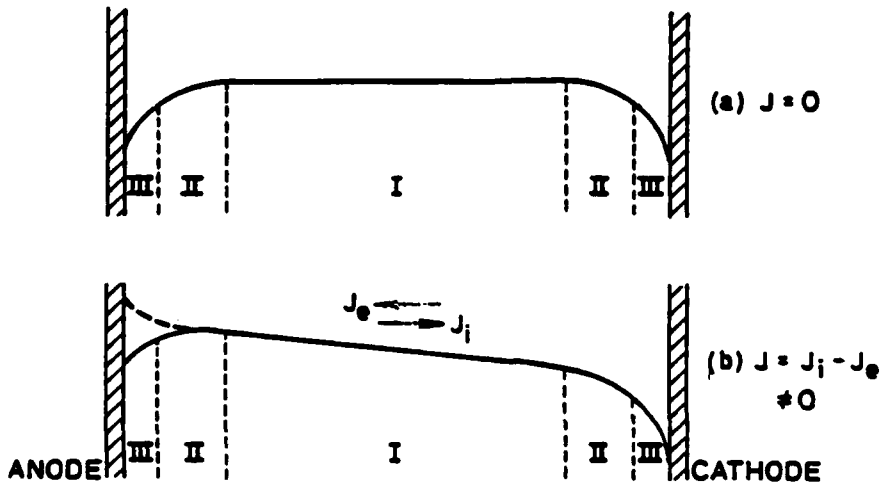

Figure 2.1. Potential distribution across plasma diode.
I Equilibrium Plasma
II Ionization Non-Equilibrium Layer
III Sheath. (Not to scale)

It should be emphasized that the four layers distinguished above are overlapping and no sharp boundaries can be distinguished. Moreover, the scale lengths are nominal ones based on freestream rather than local conditions. In general the scale lengths are ordered according to $\delta >> \ell_R >> \lambda_D \sim \ell_e \sim \ell_i$.

As the current density J is increased from zero, the potential drop at the cathode increases and more ions than electrons are collected. The reverse happens at the anode. However these conditions only hold for

very small currents $J < J_i$, the random ion current ($\lesssim 10$ mA/cm^2). For higher currents, of technical interest, the cathode must emit electrons.

At the anode it might be expected that large currents up to $J \sim J_e$, the random electron current (~ 10 A/cm^2), could be collected as a result of the reducing sheath potential drop. However it is commonly observed that constrictions in the form of anode glow spots occur at lower currents and the sheath potential drop may change sign as indicated in Figure 2.1. The reason for this behavior is unexplained hitherto.

From the foregoing discussion it is clear that the physical processes involved are extremely complex and experimental data are vital to guide the theoretical modeling.

Scientific Merit

In most plasma devices the near-electrode region and the processes by which current is transferred between the plasma and the electrodes is very poorly understood, despite the fact that the plasma-electrode interaction is frequently the performance-limiting process in the use of the device. This program is planned to shed new insight into this subject and could well result in performance improvements with respect to voltage and power losses and electrode erosion effects.

Status Report

(a) Theoretical Work

The approach adopted for theoretical modeling is to start off with the simplest relevant model and to introduce the complexities of the complete problem one at a time. To this end, the plasma-sheath problem for a plane electrode in contact with a uniform, equilibrium, weakly-ionized plasma has been formulated in some generality. By assuming that the plasma is isothermal and stationary, the complexities associated with the gasdynamic thermal boundary layer and Joule heating are, for the present, eliminated and the essential plasma physics aspects of the problem are clearly revealed.

This formulation in terms of the conservation equations for the electron and ion concentrations and momenta (including inertia), together with Poisson's equation, give a uniform description of the ionization nonequilibrium layer and sheath, in both the collionless and collision dominated regimes, without having to resort to an arbitrary division and matching of the separate regions. The governing equations have been non-dimensionalized and have been programmed for numerical solution.

In addition, an analytic solution has been derived in the quasi-neutral continuum approximation which describes the ionization nonequilibrium region exactly, and allows a number of useful explicit results to be obtained. This work is the subject of a paper [2.1] which has recently been published. The principal results are summarized below.

Expressions for the profiles of the various parameters of interest are derived in normalized form as follows.

For the plasma concentration

$$\bar{n} = \tanh \bar{y} \quad ; \tag{2.1}$$

For the net generation rate of electron-ion pairs:

$$\dot{\bar{n}} = \beta \, n_\infty^2 \operatorname{sech}^2 \bar{y} \tanh \bar{y} \quad ; \tag{2.2}$$

For the electric field:

$$\bar{E} = \left[- \operatorname{sech}^2 \bar{y} + \bar{J} \right] \coth \bar{y} \quad ; \tag{2.3}$$

For the potential:

$$\bar{\phi} = \ell n \tanh \bar{y} - \bar{J} \, \ell n \sinh \bar{y} \quad ; \tag{2.4}$$

For the charged particle fluxes:

$$\bar{\Gamma}_e = \left[-\frac{2\mu_i}{\mu_e} \operatorname{sech}^2 \bar{y} - \bar{J} \right] \quad ; \tag{2.5a}$$

$$\bar{\Gamma}_i = \left[-2 \operatorname{sech}^2 \bar{y} + \bar{J} \right] \quad . \tag{2.5b}$$

Here, the normalized distance is $\bar{y} = (y/\ell_R)$; the normalized concentration and generation rate are $\bar{n} = (n/n_\infty)$, $\bar{\dot{n}} = (\dot{n}/n_\infty)$; the normalized potential is $\bar{\phi} = (e\phi/kT)$; the normalized electric field is $\bar{E} = (E/E_R)$ where $E_R \equiv (kT/e\ell_R)$, is a characteristic electric field; the normalized current density is $\bar{J} = (J/J_R)$, where $J_R \equiv \sigma_\infty E_R$ is a characteristic current density; and the normalized fluxes are $\bar{\Gamma}_e = (\Gamma_e/n_\infty \mu_e E_R)$ and $\bar{\Gamma}_i = (\Gamma_i/n_\infty \mu_i E_R)$, respectively.

The profiles of $\bar{n}$ and $\bar{\dot{n}}$, which are independent of current are shown in Figure 2.2, while the potential profiles as a function of current density are shown in Figure 2.3.

Certain important deductions can be made concerning the behavior of the solution as a function of normalized current density. First, for a cathode ($\bar{J} < 0$), it is clear from Eq. 2.5a that when $-\bar{J}$ exceeds the relatively small value (μ_i/μ_e), the cathode must emit electrons. Second, for an anode ($\bar{J} > 0$), it follows from Eqs. 2.3 and 2.4 that the potential fall changes sign from negative to positive for $\bar{J} > 1$. Third, for an anode, it follows from Eq. 2.5b that for $\bar{J} > 2$ the anode must emit ions.

In addition, this solution in the quasi-neutral, continuum approximation has been used to evaluate the magnitude of the neglected terms in the full equations, so that the points where space charge and ion and electron inertia become significant can be determined. This enables one to derive conditions distinguishing between the cases of collisionless or collision dominated sheaths.

The chief utility of these results is to delineate the main regimes of the plasma-electrode interaction and to guide the development and interpretation of results obtained by numerical solution of the complete equations.

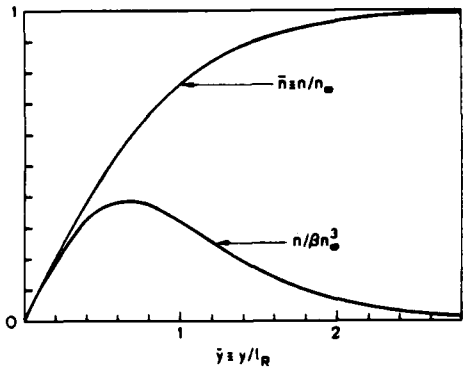

Figure 2.2. Profiles of normalized charged particle concentrations and net generation rate.

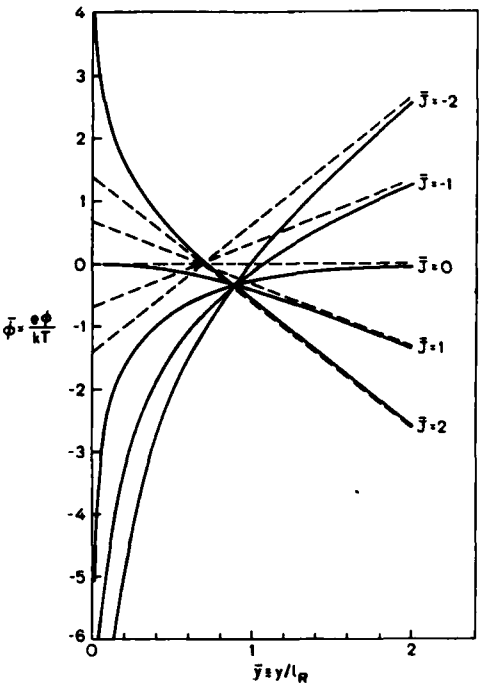

Figure 2.3. Profiles of the normalized potential as a function of normalized current density: $J < 0$, cathode; $J > 0$, anode. Broken lines indicate the asymptotes corresponding to the uniform electric field in the distant plasma

Experimental Work

The experimental work in progress is based on the use of a versatile bench-scale diffusion burner capable of producing a combustion plasma to 3000K and seeded to 1% by mass of potassium vapor to produce a thermal plasma with a conductivity of up to 10 mho/m. This facility was built in connection with an earlier NSF grant for the testing of plasma diagnostic techniques.

Currently a chimney, or flow channel, of internal cross-section 1-1/2 in. x 3-1/2 in. is being designed to fit above the flat-flame burner body. This has ceramic side-walls to reduce heat losses and so minimize the decrease in plasma temperature and conductivity with height above the burner surface.

A pair of cooled electrodes, 1 cm diameter, project from the ceramic sidewalls into the plasma flow, to give an electrode spacing adjustable between 0.5 and 1.5 cm. Electrodes of both copper and stainless steel will be used, and their cooling will be adjustable to vary the surface temperature up to within a reasonable safety margin of the respective melting points.

When the thermal design of the flow channel and electrodes has been tested and finalized, it is planned to make electrical measurements. These will be made by holding the plasma and electrode thermal conditions in a steady state and applying short (1-10 msec) voltage pulses between the electrodes at a low repetition rate. A power supply capable of delivering pulses up to 10 A at 400 V with variable pulse length and repetition rate is available for this work. The purpose of using a low duty ratio is to minimize electrode damage which is likely to be a problem under continuous energization at the power levels of interest.

Initially, the primary diagnostic technique will be to observe the voltage-current characteristic as a function of pulse duration to determine the transitions from uniform to constricted modes of current transfer. Additional diagnostic techniques such as voltage probes and fast cine recording are also being designed into the experimental set up.

2.3 Interaction of Discharges and Fluid Dynamics

Introduction

In several space power and propulsion systems of potential interest to the Air Force, such as MPD thrusters and other MHD devices, fluid motions induced by discharges are of critical importance to both the understanding and performance of the system. In any MHD device the electromagnetic field may affect the plasma flow field in several ways. Among these effects are the following:

(1) the effect of Joule heating on plasma temperatures;

(2) the Hartmann effect;

(3) turbulence suppression; and

(4) the generation of secondary flows.

The first three of these effects have been the subjects of previous studies performed at HTGL ([3.1-3.4]; these are summarized in 3.5). The fourth effect, secondary flows, is the area in which our current efforts are primarily focused. We are also continuing our investigation in the area of turbulence suppression by magnetic fields.

The physical mechanism for secondary flow in a confined plasma flow with a transverse magnetic field is illustrated in Figure 3.1. For simplicity we illustrate a distribution of the Hall current, $J_x(z)$, which one would expect from a first-order analysis. The magnetic field $\mathbf{B}=B_z$ is assumed constant. The resulting distribution of the $\mathbf{J} \times \mathbf{B}$ Lorentz force, acting as a body force against the fluid in the channel cross-plane, then causes a secondary flow field which is characterized by large-scale vortices. It is believed that the presence of this sort of transverse flow-field may have profound implications for the performance of MHD devices [3.6-3.7]. The existence of secondary flow has been inferred from data obtained at HTGL on temperature profiles, voltage drops and heat transfer [3.8].

The goals of the present work are to obtain direct measurements of the secondary flow field under conditions in which the current discharge in the Hall direction is controlled, and to correlate these results with simultaneous measurements of the axial development of the transverse electric field, which we expect to be significantly affected.

Scientific Merit

Secondary flow and the Hartmann effect are closely related, in that they are both manifestations of the appearance of the Lorentz force in the fluid momentum equation for a collision-dominated plasma,

$$\rho \frac{Du}{Dt} = - \nabla p - \nabla \vec{\tau} + \mathbf{J} \times \mathbf{B} \qquad (3.1)$$

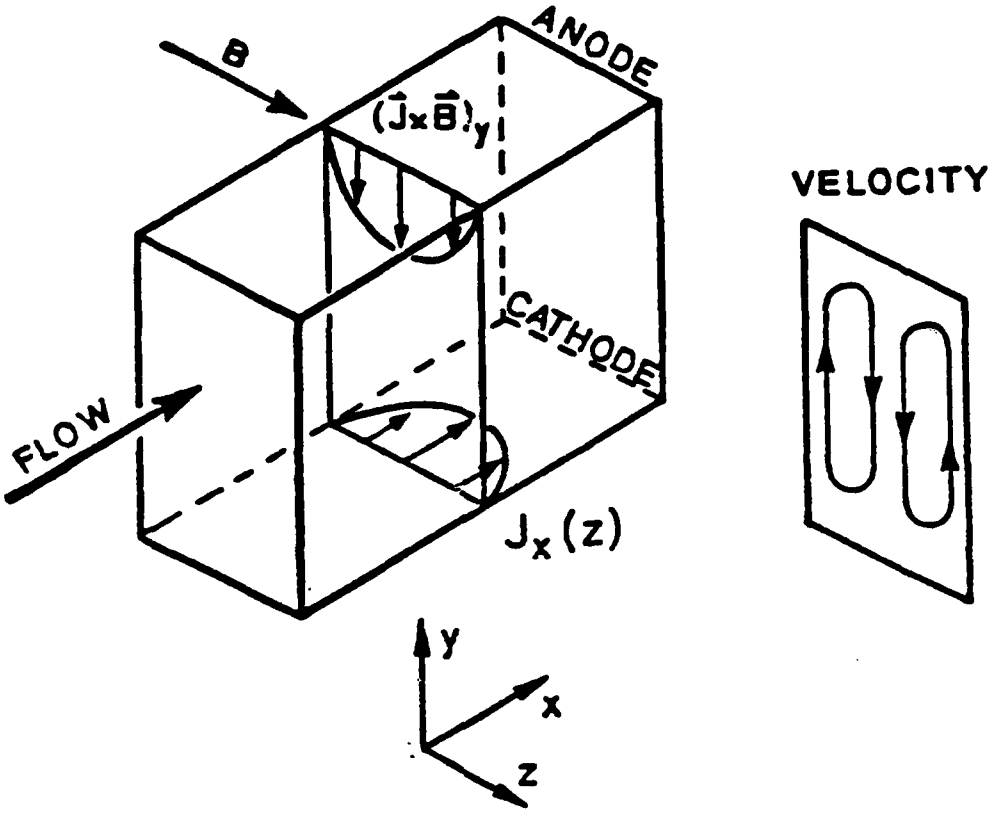

Figure 3.1. Physical mechanism for secondary flow in an MHD channel.

For a linear MHD device B is assumed to point in the z-direction; thus the Lorentz force has components in the x- and y-directions.

The axial component, J_yB, gives rise to the Hartmann effect, while the transverse component, $-J_xB$, causes secondary flow. Whereas the Hartmann effect has been of interest since Hartmann's first investigation, in 1937, it is only recently that secondary flow has received attention. The fact that theoretical models predict that secondary flow may be an important effect in real MHD devices underscores the need for

an experimental study of this phenomenon. Except for our own recent work, no measurements of MHD secondary flow velocities have been reported.

Status Report

A preliminary series of experiments was conducted at HTGL in November, 1983, in which measurements of the MHD-induced secondary flow field were obtained. These results will be reported at the 1984 IEEE International Conference on Plasma Science, to be held May 14-16 in St. Louis [3.9], and at the 22nd Symposium on Engineering Aspects of MHD, to be held June 26-28 at Mississippi State University [3.10].

The experiments were conducted at the Stanford M-2 MHD facility. The channel was connected in the Hall configuration, with an electrode pair at the upstream end of the channel connected to a pair at the downstream end; the net Hall current was controlled by means of an external power supply. Velocities were measured using laser Doppler anemometry. A schematic of the LDA system is shown in Figure 3.2. Numerous measurements of the y-directed velocity component, v, were made over a grid covering one quadrant of the channel cross-plane, and under four sets of boundary conditions:

(A) with the Faraday field E_y open-circuited, and with the magnetic field B_z having positive polarity;

(B) E_y open-circuited, magnetic field polarity reversed;

(C) E_y short-circuited, B-field positive; and

(D) E_y short-circuited, B-field negative.

In each of the four cases the same flow rate, net Hall current, and magnetic field magnitude were maintained, corresponding to an effective MHD interaction parameter of $S_u = 3.1$.

The results are summarized schematically in Figure 3.3. In all four cases the secondary flow field is characterized by large-scale vortical structures. The peak measured velocities range from 18 m/s (Case A) to

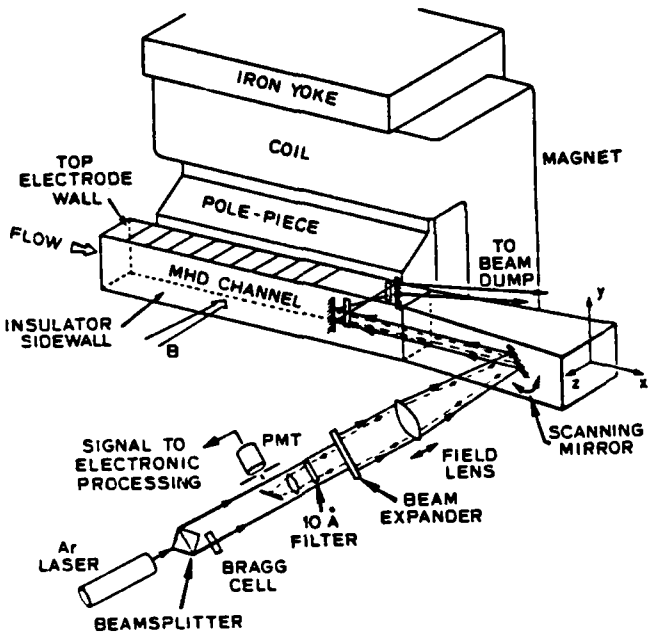

Figure 3.2. Schematic of experimental apparatus.

35 m/s (Case B); the latter corresponds to 23% of the mean axial velocity, which is far greater than the 1-2% peak secondary-flow velocities characteristic of turbulent flow through rectangular ducts in the absence of MHD effects. Figure 3.4 shows detailed results for the mean y-directed velocity measurements for one of the cases (Case B).

If we consider the simplest model for MHD-induced secondary flow, as shown in Figure 3.1, then we expect cases of positive net Hall current to lead to the sort of flow fields found in Cases B and C, in which the flow direction in the core follows the direction of the **J x B** Lorentz force, which acts as a body force on the plasma. The generation of vorticity is a consequence of the nonuniformity in this force, as can be seen by inspecting the equation for the axial vorticity, Ω_x, for the case where non-MHD sources of vorticity are neglected,

$$\rho \mathbf{u} \cdot \nabla \Omega_x = B \frac{\partial J_x}{\partial z} \tag{3.2}$$

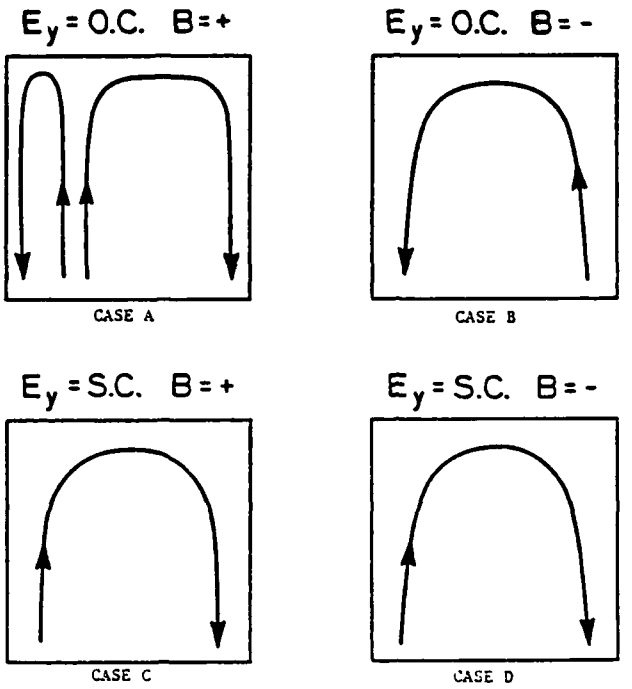

Figure 3.3. Summary of secondary flow fields measured for the four cases.

Since J_x is strongly positive in the core and goes to zero at the insulating sidewalls, a first-order analysis assumes that $\partial J_x/\partial z$ is everywhere positive over the left half of the cross-plane, and hence that Ω_x follows the sign of the B-field. The results for Cases B and C are in agreement with this expectation.

The results for cases A and D do not agree with the simple model. In Case A we observe the expected clockwise vortex in the core, but in addition there is a counter-rotating vortex in the region of the sidewall. In Case D the direction of vorticity over the entire field is opposite to the prediction of the first-order analysis. The likely hypothesis for such behavior lies in the possible presence of axial

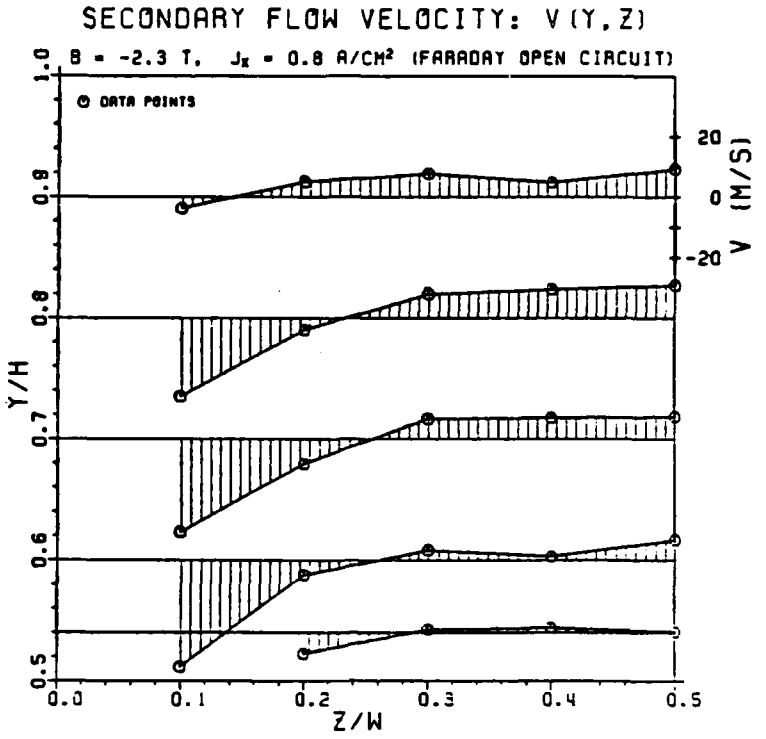

Figure 3.4. The measured secondary flow field for conditions of Case B.

velocity overshoots in the insulating wall boundary layer. This phenomenon, which is a consequence of the Hartmann effect, can lead to the presence of a region in which $\partial J_x/\partial z$ is negative even though the sign of J_x is positive in the core. This comes about because of the effect of the **u x B** field on J_x, as described by the generalized Ohm's law. That such velocity overshoots can occur in the Stanford channel was demonstrated by Rankin [3.2].

It is clear from these preliminary results that secondary flow is indeed a significant phenomenon in MHD devices. Presently an experiment is being prepared in which this line of investigation will be further pursued. In addition to demonstrating reproducibility, we expect this next experimental series to add to what we learned from the results discussed above. The following features will be incorporated:

(1) The apparatus will be modified to allow scanning over the entire cross-plane, instead of over just one quadrant. Thus we will obtain a more comprehensive picture of the secondary flow field.

(2) We will measure u(z) profiles in order to see whether our hypothesis concerning velocity overshoots may be valid.

(3) Detailed measurements will be made of plasma voltage differentials in both the axial and transverse directions. This should demonstrate the effect which secondary flows exert on the distribution of the channel electric field.

As mentioned in the introduction to this section, we are also continuing our investigation of turbulence suppression. Although the damping of plasma turbulence by a magnetic field has been demonstrated both by Olin, who used a specially-designed Pitot probe [3.3], and by Reis, who used laser Doppler anemometry [3.4], there remains an uncertainty as to whether this turbulence suppression causes a laminarization of the mean axial velocity profile; i.e., u(y) in the absence of current. Olin's data suggest that such an effect does occur; Reis's, that it does not. As the conditions for these two investigations differed, we intend to try to resolve this question by performing LDA measurements under conditions similar to those which obtained for Olin. This should allow us to determine whether his results were due to inadequacies in his measurement technique, or to differences in the flow conditions between the two experiments.

3.0 REFERENCES

1.1 Mitchner, M. and C.H. Kruger, Partially Ionized Gases. John Wiley & Sons, Inc., 1973

1.2 Kelley, R. and P.J. Padley, "Measurement of Collisional Ionization Cross-Sections for Metal Atoms in Flames," Proc. Roy. Soc, A-327, 345 (1976).

1.3 Bates, D.R., "Ionization and Recombination in Flames," Proc. Roy. Soc., A-348, 427 (1976).

1.4 Bates, D.R., V. Malaviya, and N.A. Young, "Electron-Ion Recombination in a Dense Molecular Gas," Proc. Roy. Soc., A-320, 437 (1971).

1.5 Hinnov, E., and J.G. Hirschberg, "Electron-Ion Recombination in Dense Plasmas," Phys. Rev., 125, 795 (1962).

1.6 Shapiro, A.H., The Dynamics and Thermodynamics of Compressible Fluid Flow, Vol. I. The Ronald Press Co., 1953.

2.1 Self, S.A. and L. Eskin, "The Boundary Layers Between Electrodes and a Thermal Plasma," IEEE Trans. Plasma Science, P.S. 11, 279-285 (Dec. 1983).

3.1 James, R.K. and C.H. Kruger, "Joule Heating Effects in the Electrode Wall Boundary Layer of MHD Generators," AIAA J., **21**, 679 (1983).

3.2 Rankin, R. R., S.A. Self, and R.H. Eustis, "Study of the Insulating Wall Boundary Layer in a Faraday MHD Generator, AIAA J., **18**, 1094 (1980).

3.3 Olin, J.G., "Turbulence Suppression in Magnetohydrodynamic Flows," SU-IPR Report No. 85, Department of Mechanical Engineering, Stanford University (1966).

3.4 Reis, J.C., C.H. Kruger, and S.A. Self, "Laser Doppler Velocimetry Measurements of Turbulence Suppression in a Combustion-Driven MHD Generator", in Engineering Applications of Laser Velocimetry, edited by H.W. Coleman and P.A. Pfund, New York, American Society of Mechanical Engineers, 49 (1982).

3.5 Kruger, C.H. and S.L. Girshick, "A Review of MHD Boundary Layer Research at Stanford, with Emphasis on Measurements of the Effects of Secondary Flows," 8th International Conference on MHD Electrical Power Generation, Moscow, USSR (1983).

3.6 Doss, E.D. and R.K. Ahluwalia, "Three-Dimensional Flow Development in MHD Generators at Part Load," J. Energy, 7, 289 (1983); AIAA Paper 82-0324 (1982).

3.7 Maxwell, C.D., et. al, "Three-Dimensional Effects in Large Scale MHD Generators," AIAA 14th Fluid and Plasma Dynamics Conference, Palo Alto, California, AIAA-81-1231 (1981).

3.8 Girshick, S.L. and C.H. Kruger, "Evidence of Secondary Flow in Faraday MHD Generators," 21st Symposium on Engineering Aspects of Magnetohydrodynamics, Argonne, Illinois (1983).

3.9 Girshick, S.L. and C.H. Kruger, "The Transverse Flow Field in an MHD Channel," to be presented at the 1984 IEEE International Conference on Plasma Science, May 14-16, 1984, St. Louis.

3.10 Girshick, S.L. and C.H. Kruger, "Measurements of Secondary Flow in an MHD Channel," to be presented at the 22nd Symposium on Engineering Aspects of MHD, Mississippi State, Mississippi, June 26-28, 1984.

4.0 PUBLICATIONS AND PRESENTATIONS

1. Self, S.A. and L. Eskin, "The Boundary Layers Between Electrodes and a Thermal Plasma," IEEE Trans. Plasma Science, P.S. 11, 279-285 (Dec. 1983).

2. Kruger, C.H. and S.L. Girshick, "A Review of MHD Boundary Layer Research at Stanford, with Emphasis on Measurements of the Effects of Secondary Flows," 8th International Conference on MHD Electrical Power Generation, Moscow, USSR (1983).

3. Girshick, S.L. and C.H. Kruger, "Evidence of Secondary Flow in Faraday MHD Generators," 21st Symposium on Engineering Aspects of Magnetohydrodynamics, Argonne, Illinois (1983).

4. Girshick, S.L. and C.H. Kruger, "The Transverse Flow Field in an MHD Channel," to be presented at the 1984 IEEE International Conference on Plasma Science, May 14-16, 1984, St. Louis.

5. Girshick, S.L. and C.H. Kruger, "Measurements of Secondary Flow in an MHD Channel," to be presented at the 22nd Symposium on Engineering Aspects of MHD, Mississippi State, Mississippi, June 26-28, 1984.

5.0 PERSONNEL

The following personnel contributed to this report.

Charles H. Kruger	Professor and Chairman, Department of Mechanical Engineering
Morton Mitchner	Professor, Department of Mechanical Engineering
Sidney A. Self	Professor (Research), Department of Mechanical Engineering
Stephen M. Jaffee	Research Assistant, High Temperature Gasdynamics Laboratory, Department of Mechanical Engineering
Leo D. Eskin	Research Assistant, High Temperature Gasdynamics Laboratory, Department of Mechanical Engineering
Steven L. Girchick	Research Assistant, High Temperature Gasdynamics Laboratory, Department of Mechanical Engineering

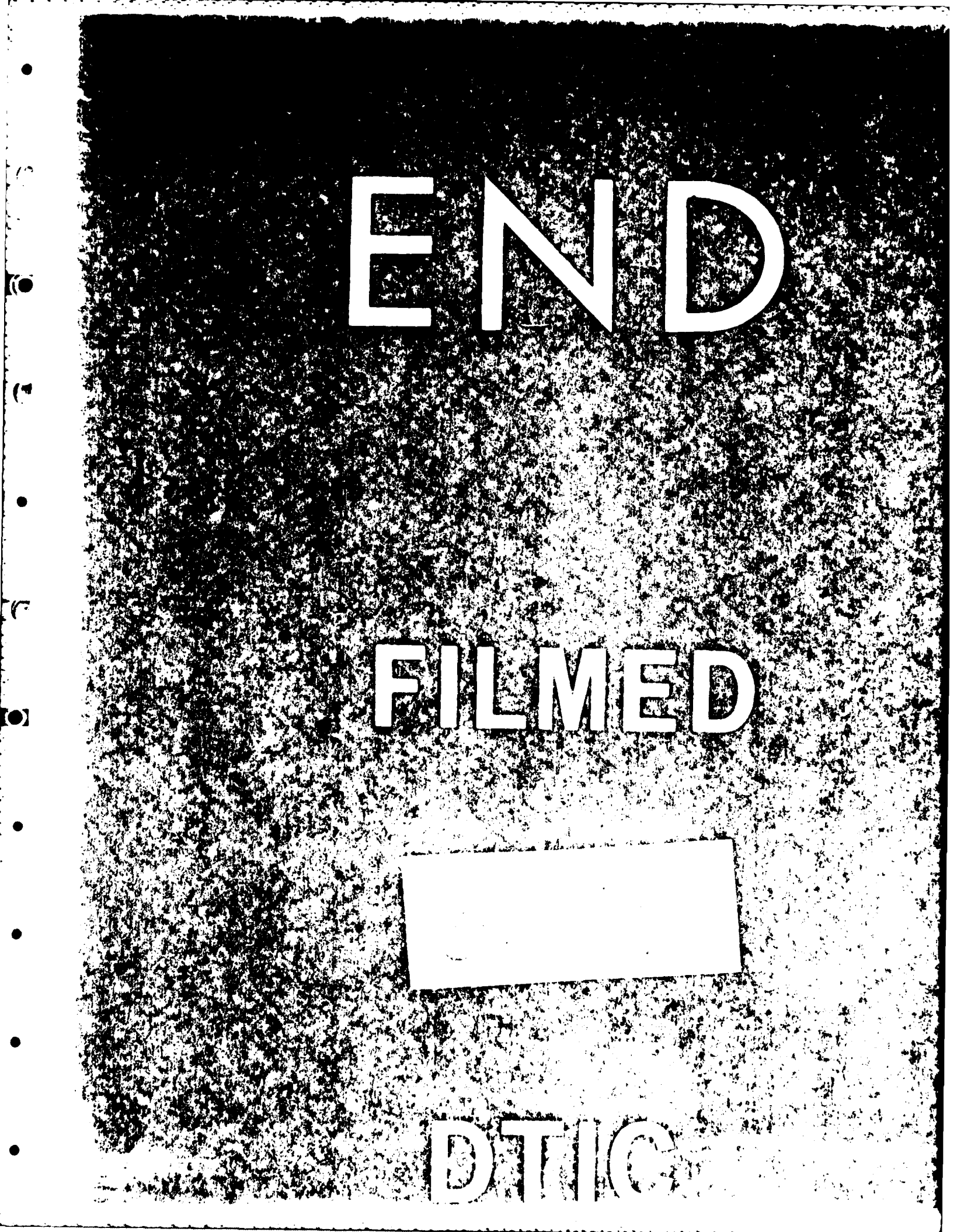
END
FILMED
DTIC